

Gas Dynamic and Transport Phenomena in the Two-Dimensional Jet Interaction Flowfield

W. J. THAYER III*

U.S. Army Air Mobility R&D Laboratory, NASA Lewis Research Center, Cleveland, Ohio

AND

R. C. CORLETT†

University of Washington, Seattle, Wash.

Pressure, temperature, gas sampling, and optical measurements were made in the turbulent separated flow region upstream of jets. Hot hydrogen, helium, and nitrogen were injected from a converging slot nozzle perpendicular to the heated Mach 2.5 airstream above a flat plate. The dependence of the separation distance, wall pressure, and side force on the jet to freestream pressure and density ratios and the separation Reynolds number was determined. The injectant concentration in the separated flow region was found to be high, and to correlate with a ratio of the injectant and freestream temperatures and molecular weights. A tracer gas injection technique was used to determine air and injectant mass transport rates through the separated flow region. Approximately five percent of the gas injected passed through this region.

Nomenclature

A_c	= amplification factor
c	= sonic velocity
d	= slot width
F	= force or thrust
h	= height of jet or step
ℓ	= distance from leading edge of model
L	= distance from leading edge to slot nozzle
M	= Mach number
m	= mass
\dot{m}	= mass flow rate
P	= dimensionless flowfield property
p	= pressure
R_i	= gas constant for species i
Re_ℓ	= Reynolds number based on length = $\rho_a u_a \ell / \mu_a$
Re_x/x	= unit Reynolds number = $\rho_a u_a / \mu_a$
s	= jet or step span
T	= absolute temperature
u	= velocity parallel to the plate
V	= volume
\dot{V}	= volume flow rate
W	= mass flux ratio
w	= mass flux
x	= axial distance, from slot nozzle or step face, positive upstream
Y_i	= mass fraction of species i
α	= boundary-layer separation angle
γ	= specific heat ratio
μ	= absolute viscosity
ρ	= density

Subscripts

a	= property of the wind-tunnel airstream at $M = 2.5$
ar	= air passing through the upstream recirculation region
e	= property at jet nozzle exit
j	= jet or injectant
jr	= injectant passing through the upstream recirculation region
jv	= related to a jet exhausting into a vacuum
oa	= air stagnation condition

Presented as Paper 71-561 at AIAA 4th Fluid and Plasma Dynamics Conference, Palo Alto, California, June 21-23, 1971; submitted July 8, 1971; revision received November 23, 1971. This paper is based on the Ph.D. dissertation submitted by W. J. Thayer to the Mechanical Engineering Department, University of Washington. This research was supported by the Boeing Scientific Research Laboratories.

Index categories: Boundary Layers and Convective Heat Transfer—Turbulent; Jets, Wakes, and Viscid-Inviscid Flow Interactions; Hypersonic Airbreathing Propulsion.

* Research Engineer; formerly Basic Research Associate, Boeing Scientific Research Laboratories, Seattle, Wash. Associate Member AIAA.

† Associate Professor, Department of Mechanical Engineering. Member AIAA.

oj	= jet stagnation condition
p	= plateau
s	= jet normal shock, or computed nozzle width
sep	= separation
ss	= start of the separation pressure rise
t	= tracer gas
1.5	= location at which $p/p_a = 1.5$

Introduction

INJECTION of secondary jets into a supersonic stream is of interest for thrust vector control, hypersonic vehicle control, and supersonic combustion applications. This paper deals with the interaction of a highly underexpanded jet with a Mach 2.5 airstream. The converging slot nozzle used in this experimental investigation was oriented perpendicular to the primary stream. This gas injection process is referred to as "transverse injection," and the corresponding flow as the "jet interaction flowfield." Transverse injection causes separation of the boundary layer upstream of the jet, as depicted in Fig. 1a. The wall pressure distribution characteristic of the turbulent flow studied, and some associated terminology, are shown in Fig. 1b.

Properties of upstream separated flow regions which are important in both supersonic combustion and hypersonic vehicle control were investigated. These properties include the heat and mass transfer characteristics of the separated flow region and the effect of widely variable air and injectant temperatures on the flow geometry and transport characteristics. Although transverse injection from slot nozzles has been studied extensively during the

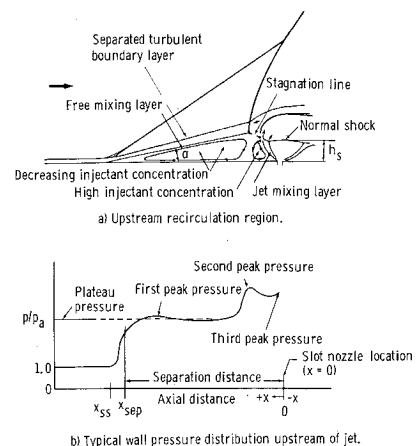


Fig. 1 Upstream recirculation region of the jet interaction flowfield.

past decade,¹⁻⁴ almost no data of this nature are available. Most previous work has been directed at determining the wall pressure distribution and flow geometry for jet interaction control applications, and has utilized ambient temperature air and injectant streams. In the present work, the air stream temperature and pressure, the injectant temperature and pressure, and the species injected were independently variable. This capability has made possible a systematic investigation of the dependence of the separation region wall pressure distribution, chemical composition, temperature, and mass transport rates on several controllable parameters. A "well mixed" model of the separated flow region is proposed and used, in conjunction with the concentration and flow measurements, to determine the mass transport rates in this region. The results suggest that the separated flow region will control spontaneous ignition at sufficiently high temperature, as has been observed in subsequent experiments.⁵

A "Well-Mixed" Model of the Separated Flow Region

A novel experimental technique was used to estimate the mass transport rates of air \dot{m}_{ar} , and injectant \dot{m}_{jr} , through the recirculation region upstream of a transverse jet. The basis of this technique is the assumption that the recirculation region is "well mixed," as defined below. This assumption makes possible the evaluation of the ratio of the air and injectant transport rates, $\dot{m}_{ar}/\dot{m}_{jr}$, from the composition. A second assumption makes possible an approximate experimental determination of the magnitudes of \dot{m}_{ar} and \dot{m}_{jr} .

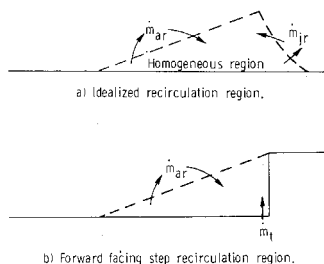


Fig. 2 Control volumes used for transport considerations.

Gas particles that enter the separated flow region circulate within this region for some time before turbulent transport sweeps them out and replaces them. Air enters the recirculation region at the rate, \dot{m}_{ar} , through the separated boundary layer by a turbulent mixing process, Fig. 2. Injectant enters the region through the jet shear layer by a similar process. A mixture of injectant and air of equal mass simultaneously leaves the region through these mixing layers. The key assumption of this flow model is that, as gas enters the recirculation region, it mixes with the gas already there in a period of time which is short compared with the characteristic residence time. A recirculation region exhibiting this behavior is called well mixed in the remainder of this discussion. This concept is very similar to that proposed by Longwell et al.⁶ for recirculation zones downstream of bluff body flameholders, and later used to develop the "perfectly stirred reactor" for making over-all reaction rate measurements.⁷ Chemical homogeneity in the recirculation zone is a reasonable criterion for the validity of the well-mixed assumption, since perfect homogeneity would characterize the limiting case of instantaneous mixing. Since the flow is steady in the mean, the mixture in the recirculation region reflects the relative transport rates of injectant and air through the region. The mass fraction of injectant in this well-mixed region is proportional to the mass flow rates of injectant and air through the region, i.e.,

$$Y_j = \dot{m}_{jr}/(\dot{m}_{jr} + \dot{m}_{ar}) = (1 + \dot{m}_{ar}/\dot{m}_{jr})^{-1} \quad (1)$$

Thus, gas samples from a well-mixed recirculation region can be used to calculate $\dot{m}_{ar}/\dot{m}_{jr}$. From an independent determination of either one of \dot{m}_{ar} or \dot{m}_{jr} , this result can be used to determine the magnitude of the other.

The independent experiment originally chosen to quantify the mass transport rates consisted of bleeding tracer gas into the recirculation region at a known rate, taking gas samples to determine the mass fraction of tracer in the region, and using Eq. (1) to evaluate the ratio of the total mass transport rate to the known tracer gas transport rate. However, the small size and complexity of the wind-tunnel model used in this experiment prohibited uniform tracer gas injection upstream of the jet.

The physical similarity between the separated flow regions upstream of transverse jets and forward facing steps has been frequently discussed in the literature,^{3,8} and suggested another approach for determining the transport rates. It was assumed that the average mass flux of air, w_{ar} , transported across the separated turbulent boundary layer upstream of a jet is equal to that upstream of the forward facing step which results in the same separation region geometry at identical freestream conditions. The air mass transported across the separated boundary layer upstream of a step (see Fig. 2) can be evaluated by metering tracer gas into the recirculation region and sampling the resulting mixture. For this case, Eq. (1) can be rewritten as

$$\dot{m}_{ar}/\dot{m}_t = 1/Y_t - 1 \quad (2)$$

Since \dot{m}_t and Y_t can be measured through a wide range of conditions, the dependence of \dot{m}_{ar} on the freestream parameters and separated flow region size may be evaluated. The average mass flux of air across the mixing layer may be calculated if the separated flow geometry is measured. The width of the mixing layer is equal to the step span s and since the separation angle is small, the length is approximately the distance from the jet or step to the start of the separation pressure rise, x_{ss} (see Fig. 1). The average mass flux, w_{ar} , is conveniently nondimensionalized by dividing by the freestream mass flux, $\rho_a u_a$, giving

$$W_{ar} = w_{ar}/\rho_a u_a = (\dot{m}_{ar}/x_{ss}s)/\rho_a u_a \quad (3)$$

The dependence of this dimensionless mass flux on the freestream conditions was determined by using the tracer gas injection technique to evaluate the air mass transport rate. Once this dependence had been determined, the injectant mass transport rate through the recirculation region upstream of a jet could be estimated from measurable quantities. Using Eq. (3) to evaluate the air mass flow rate in Eq. (1), the injectant mass flow rate is

$$\dot{m}_{jr}(T, p, x_{ss}) = W_{ar}(T, p, x_{ss})x_{ss}s\rho_a u_a/(1/Y_{inj} - 1) \quad (4)$$

Experimental Apparatus and Measurement Techniques

This investigation was carried out in the Mach 2.5 supersonic combustion wind tunnel at the Boeing Scientific Research Laboratories.⁹ Air was heated in an alumina pebble bed storage heater to stagnation temperatures from ambient to 2550°R at stagnation pressures from 39 to 100 psia. Temperature was measured with a double platinum shielded, aspirated, platinum-platinum 13% rhodium thermocouple located in the wind-tunnel settling chamber.

The flat plate wind tunnel model used in this investigation spanned the 4-in. dimension of the 4-in. \times 6-in. test section. The 0.0080-in. wide slot nozzle was oriented perpendicular to the external stream and spanned the center 2.00 in. of the model, 5.00 in. from the leading edge. Side plates enclosed the 2.00-in. wide interaction region. Three-dimensional roughness elements were used to trip the boundary layer. At the separation point, the boundary layer was always turbulent and approximately 0.10-in. thick as determined from shadowgraphs. Arrays of static pressure taps were located upstream and downstream of the slot nozzle. Five chromel-alumel thermocouples were spot welded to the underside of the thin, uncooled flat plate upstream of the nozzle.

An electric gas heater provided nitrogen, helium, or hydrogen at temperatures to 2450°R and pressures from 20 to 270 psia. Injectant volume flow rates were measured to within 1% of the total volume flow rate using Potter and Flow Technology turbine flowmeters. The separated flow region composition was determined by gas chromatographic analysis of gas samples taken

through taps both on and above the plate surface. Shadowgraph pictures were taken of the jet interaction region with and without transparent sideplates. The jet normal shock height and the separation shock wave location and angle were scaled from these photographs. The wind-tunnel model, hydrogen heater, the instruments and methods used to record data during wind-tunnel runs, and the techniques for data reduction are discussed in detail in Ref. 10.

Experimental Results

Dimensional analysis shows that an appropriately nondimensionalized property P of the jet interaction flowfield depends on a set of dimensionless groups as follows:¹⁰

$$P = f[Re_L, Ma, \gamma_a, M_j, \gamma_j, (p_{oj}/p_a), (R_j T_{oj}/R_a T_a), d_j/L] \quad (5)$$

The fixed geometry of the wind tunnel and model assured that the freestream and jet Mach numbers, Ma and M_j , and the ratio d_j/L remained constant. Independent variation of the injectant temperature and pressure and the freestream temperature and pressure, using nitrogen, helium, and hydrogen as injectants, made possible determination of the dependence of flowfield properties on Re_L , p_{oj}/p_a , $R_j T_{oj}/R_a T_a$, γ_a , and γ_j . The results of this investigation follow.

Gas Dynamic Phenomena

The distance upstream of the slot nozzle at which separation occurs, subsequently referred to as the separation distance, and the plateau pressure level within the separated flow region were the properties chosen to characterize the jet interaction flowfield. Their dependence on the controllable parameters was extensively investigated. In addition, the amplification factor [defined by Eq. (7) below] was evaluated at all conditions.

Effects of pressure ratio variation

The dependence of the jet interaction flowfield on the ratio of the jet stagnation pressure to the freestream static pressure, p_{oj}/p_a , has occupied at least part of the attention of most previous investigators.^{1,3,4} Previous investigations have generally utilized ambient temperature air and injectant gases and results related to pressure ratio variation exhibit rough agreement. As has been discussed in Ref. 12, the dependence of side force, amplification factor, and separation distance on p_{oj}/p_a found during the ambient temperature part of this investigation agrees well with previous experiments.^{3,11} The variable temperature experiments reported here demonstrate that the separation distance and amplification factor have the same functional dependence on p_{oj}/p_a throughout the range of conditions investigated. The separation distance dependence on the pressure ratio is readily seen in Fig. 3, in which results for nitrogen, helium, and hydrogen injection are compared at identical freestream and injectant conditions. Since no simple, accurate method of determining the separation point is available, the distance upstream of the jet at which the plate pressure had increased to 1.5 times the freestream pressure, denoted by $x_{1.5}$, was used to represent the separation distance. As discussed in Ref. 10, this location is very near the separation point. The separation distance dependence on p_{oj}/p_a is correlated by the relation

$$x_{1.5}/d_s = a(p_{oj}/p_a)^{0.77} \quad (6)$$

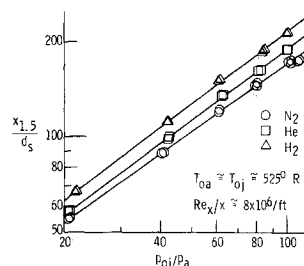


Fig. 3 Correlation of separation distance dependence on the jet to freestream pressure ratio.

The coefficient a depends on the injectant and freestream densities and the freestream Reynolds number. A power law dependence was anticipated, in view of previous observations indicating that the separation distance is related to the jet shock height,^{1,11} and that a similar relation describes the shock height of a jet expanding into quiescent surroundings.¹³ The upstream wall pressure distribution was integrated over the interaction area to evaluate the interaction force, F_i (see Ref. 10 for a detailed discussion of the data reduction procedures). The amplification factor A_c was computed from the measured interaction force and injectant mass flow rate m_j using the relation

$$A_c = (F_i + F_j)/F_{jv} = [F_i + m_j c_e + A_e(p_e - p_a)]/(m_j c_e + A_e p_e) \quad (7)$$

where F_j and F_{jv} are the thrusts of sonic jets exhausting to the freestream static pressure and into a vacuum, respectively. The sonic velocity, c_e , and the exit pressure, p_e , were calculated at the nozzle exit assuming isentropic flow. Throughout the range of temperatures, pressures, and injectants investigated, the dependence of A_c on p_{oj}/p_a is essentially identical to that determined in the cold flow experiments reported earlier, Ref. 12. The data are correlated by the relation

$$A_c = b - 0.2 \ln(p_{oj}/p_a) \quad (8)$$

The coefficient b depends on the ratio, $R_j T_{oj}/R_a T_a$, in a manner which is discussed in the next section. The amplification factor, and hence the coefficient, b , does not depend on the freestream Reynolds number in the turbulent regime of this investigation. This dependence of A_c on the pressure ratio is almost identical to that reported by Werle et al.¹¹ for injection of air into a Mach 4 airstream.

Effects of variation in density or the ratio $R_j T_{oj}/R_a T_a$

The parameter, $R_j T_{oj}/R_a T_a$, was independently varied by changing either the injectant temperature, the freestream temperature, or the species injected. Since the pressure ratio was held constant, variation of $R_j T_{oj}/R_a T_a$ is equivalent to changing the jet to freestream density ratio. Helium was usually injected to eliminate effects resulting from injectant specific heat ratio changes. Nitrogen and hydrogen were injected at several conditions to increase the $R_j T_{oj}/R_a T_a$ range.

The separation distance increases with $R_j T_{oj}/R_a T_a$ when low density gas is injected, as may be seen in Fig. 4, while the plateau pressure changes only slightly. Associated with this increase is a proportionate increase in A_c . The variation of these flow characteristics with molecular weight, as reported earlier by the author,¹² and with T_{oj} and T_a , correlate when $R_j T_{oj}/R_a T_a$ is used as the independent variable. This density dependence is not observed when high molecular weight, low-temperature gases are injected.

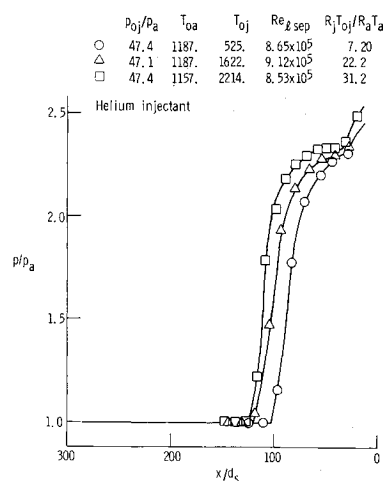


Fig. 4 Comparison of wall pressures at several values of the ratio $R_j T_{oj}/R_a T_a$.

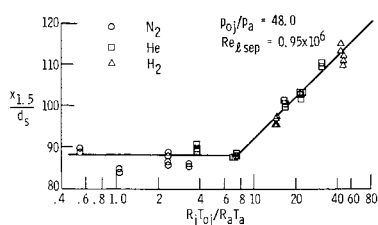


Fig. 5 Dependence of the separation distance on temperature and molecular weight.

Two distinct regimes are evident, as seen in Fig. 5. The separation distance, side force, and amplification factor are almost independent of molecular weight and temperature when $R_j T_{oj}/R_a T_a$ is less than approximately 7. This has previously been observed by Spaid,¹⁴ Spaid and Zukoski,³ and Allan¹⁵ in ambient temperature experiments utilizing several high molecular weight injectants. However, these investigators did not operate in the high $R_j T_{oj}/R_a T_a$ regime. Each of these investigators found that helium exhibited a peculiar behavior; both the separation distance and side force were greater than those found with high molecular weight injectants. On the basis of a semiempirical analysis, Spaid and Zukoski³ concluded that this increase was an effect of the injectant specific heat ratio γ_j . Allan¹⁵ demonstrated that γ_j variation does not affect the jet interaction flowfield, and concluded that a molecular weight effect was responsible for the increase. Confirming results are presented later in this paper. A variable temperature experiment has not previously been reported in the high $R_j T_{oj}/R_a T_a$ regime. Allan refers to unpublished data from a slot injection experiment employing air as the injectant. These experiments showed no change in side force when high temperature air was injected. This is not surprising, however, since the data of this experiment indicate that air must be heated to approximately 2200°R before a separation distance increase is noticeable. This was not possible in the experiment referred to by Allan.¹⁵ No slot injection experiments with hydrogen have previously been reported. Figure 5 and similar data obtained at other conditions demonstrate that as $R_j T_{oj}/R_a T_a$ increases above approximately 7, the separation distance rapidly increases. The only previous observations in this regime are the isolated data points for cold helium injection.^{3,15} These results agree with the behavior observed in this experiment. These results show that, in addition to the high density regime in which the flowfield is independent of $R_j T_{oj}/R_a T_a$, a second regime exists in which the separation distance and amplification factor depend strongly on temperature and the injectant molecular weight.

Spark shadowgraphs were taken of the interaction region to elucidate the mechanism of the separation distance dependence on $R_j T_{oj}/R_a T_a$. Since plexiglass sideplates were used during these runs, shadowgraphs were made only of ambient total temperature flows. A comparative study of hydrogen and nitrogen injection was made. The average distance measured from the jet to the intersection of the extrapolated separation shock with the plate agrees well with the location of the separation pressure rise determined from the wall pressure data. The separation shock wave angle does not depend on the gas injected. The jet normal shock heights of equal pressure ratio hydrogen and nitrogen jets are almost identical. The separation distance increase with $R_j T_{oj}/R_a T_a$ is definitely not due to an increase in the jet normal shock height. The only substantial differences between shadowgraphs of the hydrogen and nitrogen injection flowfields are in the regions immediately above the jet normal shock and downstream of the jet. These regions are always significantly larger when hydrogen is injected. As a result, the separated boundary layer appears to pass over the jet further from the plate when hydrogen is injected.

The increased size of the separated flow region seems to result from a displacement of the external stream due to the increased volume flow rate of injectant associated with high temperature and low molecular weight gas injection. Indeed, the volumetric flow rate of injectant is proportional to the product, $R_j T_{oj}$. Thus,

the increased separation distance may result from the larger jet plume that results when low-density gas is injected. However, other mechanisms may be responsible. As will be seen in the transport phenomena section, the volumetric flow rate of injectant into the separated flow region also increases when low-density gas is injected. Thus, transport of the injectant out of the upstream region could also increase the effective jet height and increase the separation distance. Existing semiempirical theories^{3,8} do not explain the observed separation distance increase. A quantitative explanation of this phenomenon awaits a more rigorous analysis of this complex flowfield.

Effects of Reynolds number variation

The freestream unit Reynolds number was varied independently of the other dimensionless groups in Eq. (5) during this phase of the investigation. This was accomplished by changing the freestream temperature. The injectant temperature was adjusted so that the ratio $R_j T_{oj}/R_a T_a$ was held constant. The ratio p_{oj}/p_a was maintained at approximately 85. Helium was usually injected to assure that changes in the injectant specific heat ratio would not complicate interpretation of results. Nitrogen was also injected at all conditions throughout the Reynolds number range investigated.

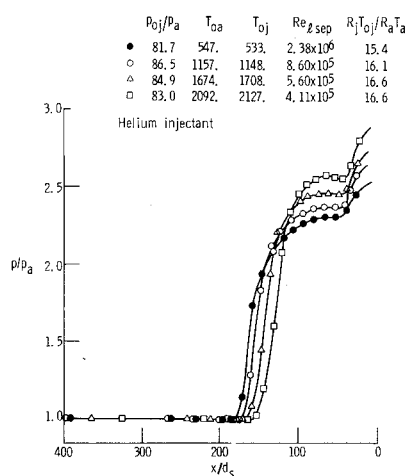


Fig. 6 Comparison of wall pressure at several values of $Re_{\delta_{sep}}$ for helium jets with other parameters constant.

Both the separation distance and the plateau pressure change with the Reynolds number, as seen in Fig. 6. As the freestream Reynolds number increases, the plateau pressure decreases. Significantly, the plateau pressure is not affected by the gas injected. Data, like those in Fig. 6, taken with hydrogen, helium, and nitrogen at the same pressure ratio and unit Reynolds number, but at many values of $R_j T_{oj}/R_a T_a$, show almost identical plateau pressures. Indeed, data taken at conditions resulting in rapid combustion of hydrogen in the region upstream of the jet demonstrate that the plateau pressure is affected very little by rapid chemical heat release.⁵ In addition to varying with freestream Reynolds number, the plateau pressure was found to change slightly with any parametric variation which resulted in a separation distance change. When correlated with the Reynolds number based on the distance from the leading edge to the separation point, $Re_{\delta_{sep}}$, all of the plateau pressure data fall on very nearly the same curve. This curve is seen in Fig. 7, and shows a plateau pressure dependence on the separation Reynolds number which is almost identical to that found by Chapman et al.¹⁶ upstream of forward facing steps. Plateau pressure data obtained upstream of forward facing steps during the mass transport experiments of this investigation are plotted in Fig. 7. The constant plateau pressure found by Love¹⁷ for fully turbulent boundary-layer separation upstream of forward facing steps at Mach 2.5, and the point reported by Hahn¹⁸ at Mach 2.5, are plotted for comparison. Plateau pressures at Mach 2.5 were interpolated

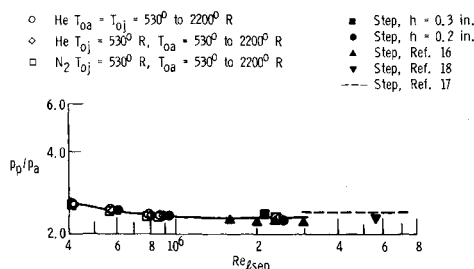


Fig. 7 Dependence of separation region plateau pressure on the separation Reynolds number for a Mach 2.5 freestream.

between the data of Chapman et al.¹⁶ at Mach 2.4 and 2.7 for turbulent boundary-layer separation upstream of forward facing steps, and also correlated with the separation Reynolds number. The plateau pressures upstream of jets and forward facing steps are very nearly identical. The ratio of plateau to freestream pressure decreases as the separation Reynolds number rises, and approaches a value of approximately 2.4 at a separation Reynolds number of 2.5×10^6 for a Mach 2.5 stream. It is evident that assuming the plateau pressure to be independent of Reynolds number, as done by Spaid and Zukoski,³ is accurate at sufficiently high Reynolds numbers. Both the jet interaction data and the forward facing step data support the conclusion that the "free interaction" model¹⁶ relates the wall pressures in the separated flow regions upstream of various obstacles, and that the plateau pressure is correlated by the separation Reynolds number when the freestream Mach number is constant.

The separation distance and wall pressure level vary simultaneously with Reynolds number in such a way (Fig. 6) that the amplification factor is almost independent of the Reynolds number, as seen in Fig. 8. The results for nitrogen and helium injection are very similar, and indicate a very slight increase in amplification factor with Reynolds number. However, the increase seen in Fig. 8 is not experimentally significant. This result agrees very well with results reported by Werle⁸ indicating no change in amplification factor through a limited Reynolds number range. No data are available to suggest any sensitivity of the amplification factor to freestream Reynolds number changes.

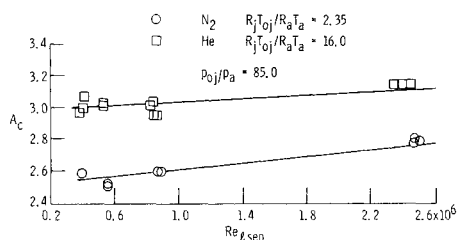


Fig. 8 Variation of the amplification factor with the Reynolds number at separation.

Effect of injectant specific heat ratio

A few wind-tunnel runs were made to examine the effect of changing the injectant specific heat ratio, γ_j . The effect of γ_j variation was studied by injecting hydrogen ($\gamma_j = 1.4$) and helium ($\gamma_j = 1.67$) at conditions for which the other important parameters could be matched. Wall pressure distributions typical of this experiment are seen in Fig. 9. The difference between these two curves is very small. The semiempirical flow models of Spaid and Zukoski,³ and recently of Werle et al.⁴ predict a separation distance increase of approximately 20% when γ_j increases from 1.4 to 1.67. The results of this investigation demonstrate that the separation distance, plateau pressure, and amplification factor do not increase with the injectant specific heat ratio. Although not generally recognized, this result was previously demonstrated by Allan,¹⁵ who maintained a nominally constant $R_j T_{0j}/R_a T_a$ by injecting nitrogen ($\gamma_j = 1.4$, $R_j = 28$) and ethane ($\gamma_j = 1.22$, $R_j = 30.1$) in a cold flow experiment.

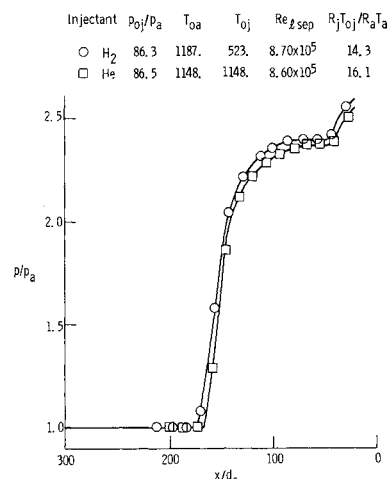


Fig. 9 Comparison of wall pressures for hydrogen and helium injection at constant $R_j T_{0j}/R_a T_a$.

Effect of free stream specific heat ratio

The importance of the freestream specific heat ratio, γ_a , was also checked. Conceivably, since γ_a depends on temperature, variation of this parameter might be important for the range of temperatures investigated. To determine the magnitude of this effect, the freestream temperature was doubled (γ_a changed from 1.40 to 1.32) and the other parameters were adjusted to preserve the Reynolds number, pressure ratio, and $R_j T_{0j}/R_a T_a$. Flowfield changes due to this variation seem to be small, but measurable. The plateau pressure increases slightly (approximately 2%) as γ_a decreases from 1.40 to 1.32, but the separation distance remains approximately constant.

Transport Phenomena

Recirculation region composition

Analyses of gas samples withdrawn from the recirculation region through pressure taps demonstrate that the axial distribution of injectant in the recirculation region is similar to the wall pressure distribution. Regions of slowly increasing injectant concentration, much like the pressure plateau, are present. These will be referred to as "concentration plateaus." The wall pressure approaches the plateau pressure level a short distance downstream of the separation point. The concentration plateau is approached in a similar manner, but the distance from the separation point to the start of the concentration plateau is approximately twice the corresponding distance associated with the pressure rise. The region of nearly uniform composition encompasses the major portion of the larger recirculation regions observed. The fraction of injectant in this region is high, a mole fraction near 40% being typical for hydrogen injection.

The composition of the recirculation region is insensitive to variation of any parameter except the ratio, $R_j T_{0j}/R_a T_a$. Figure 10 shows the correlation of the mass fraction of the injectant at the concentration plateau, Y_p , for all of the wind tunnel runs made during this investigation. This correlation is well described by the relation

$$Y_p = 0.23(R_j T_{0j}/R_a T_a)^{-1/2} \quad (9)$$

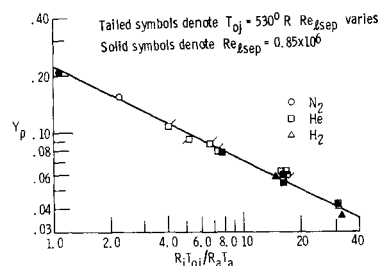


Fig. 10 Correlation of the plateau mass fraction with the ratio $R_j T_{0j}/R_a T_a$.

which is drawn through the data in Fig. 10. To the authors' knowledge, there exist no published results with which these data may be compared.

Mass transport rates

The ratio of the injectant and air transport rates through the recirculation region can be calculated from composition measurements using Eq. (1). The existence of a large, almost homogeneous, portion of the recirculation region lends substantial support to the well-mixed assumption on which Eq. (1) is based. A tracer gas injection experiment, also based on this assumption, was carried out to determine the mass flux of air across the separated turbulent boundary layer. Helium tracer gas was injected into the recirculation region upstream of forward facing steps. These experiments were conducted through a range similar to that covered in the transverse injection investigation. The tracer gas was metered and injected from ten small tubes evenly spaced across the model just upstream of the step. Gas sampling and wall pressure measurements were made as in the jet interaction experiments. These data were used in Eq. (2) and (3) to evaluate the dimensionless transport mass flux through the separated boundary layer W_{ar} . Within the accuracy of this investigation, this quantity remained constant and equal to 0.023. This result was used in Eq. (4), with the flowfield properties measured in the jet interaction experiments, to evaluate the injectant mass transport rate into the recirculation region. The estimated injectant transport rates are plotted in Fig. 11 as the fraction of the total injectant mass flow rate \dot{m}_j . The data presented in Fig. 11 represent the entire range of conditions examined during this investigation. Approximately 5% of the gas injected passes through the recirculation region. This fraction decreases as the ratio of the air to injectant temperature increases.

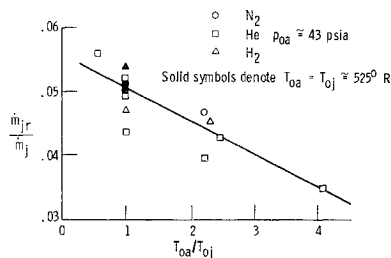


Fig. 11 Estimated injectant mass flow rates through the upstream recirculation region.

Conclusions

The effects of independent variation of p_{0j}/p_a , $R_j T_{0j}/R_a T_a$, γ_j , γ_a , and the freestream Reynolds number have been determined. The separation distance, plateau pressure, and amplification factor are significantly affected by changes in p_{0j}/p_a and $R_j T_{0j}/R_a T_a$, but very little by variation of the freestream Reynolds number. The jet to freestream pressure ratio has a very strong effect on the size of the upstream separated flow region. The dependence of the separation distance on p_{0j}/p_a is correlated by Eq. (6). The ratio of plateau to freestream pressure decreases and the separation distance increases as the Reynolds number rises. The former approaches a value of approximately 2.4 at very high separation Reynolds numbers. The net effect of a Reynolds number change on the interaction force and the amplification factor is very small. The jet temperature and molecular weight strongly influence the separation distance when low molecular weight or high-temperature gases are injected. This effect is correlated by the ratio $R_j T_{0j}/R_a T_a$. Two regimes of dependence on this parameter are found. At values of $R_j T_{0j}/R_a T_a$ below 7, the separation distance is not affected by changes in this parameter. As $R_j T_{0j}/R_a T_a$ is increased above 7, the separation distance rapidly increases, causing a similar increase in side force and amplification factor. Changes in γ_j and γ_a have little effect on the flowfield.

The separated flow region has a high injectant concentration at all conditions investigated. A concentration plateau, similar to the wall pressure plateau, occurs in the separated flow region. The mass fraction of injectant at the concentration plateau correlates with the parameter, $R_j T_{0j}/R_a T_a$, alone, as expressed in Eq. (9). The fact that a large portion of the recirculation region has this nearly uniform, plateau concentration supports the well-mixed flow model. The dimensionless transport mass flux across the separated boundary layer, $W_{ar} = \dot{m}_{ar}/x_{ss}\rho_a u_a$, is approximately constant and equal to 0.023. Approximately 5% of the mass injected from the slot nozzle passes through the upstream recirculation region.

References

- 1 Sterrett, J. R. and Barber, J. B., "A Theoretical and Experimental Investigation of Secondary Jets in a Mach 6 Free Stream with Emphasis on the Structure of the Jet and Separation Ahead of the Jet," TM X-57137, 1966, NASA.
- 2 Hawk, N. E. and Amick, J. L., "Two-Dimensional Secondary Jet Interaction with a Supersonic Stream," *AIAA Journal*, Vol. 5, No. 4, April 1967, pp. 655-660.
- 3 Spaid, F. W. and Zukoski, E. E., "A Study of the Interaction of Gaseous Jets from Transverse Slots with Supersonic External Flow," *AIAA Journal*, Vol. 6, No. 2, Feb. 1968, pp. 205-212.
- 4 Werle, M. J., Driftmyer, R. T., and Shaffer, D. G., "Jet-Interaction-Induced Separation of Supersonic Turbulent Boundary Layers—The Two Dimensional Problem," AIAA Paper 70-765, Los Angeles, Calif., 1970.
- 5 Thayer, W. J., III and Corlett, R. C., "Ignition and Combustion of a Transverse Hydrogen Jet in a Mach 2.5 Airstream," Paper WS/CI-71-15, April 1971, Western States Section/The Combustion Inst., Denver, Colo.
- 6 Longwell, J. P., Frost, E. E., and Weiss, M. A., "Flame Stability in Bluff Body Recirculation Zones," *Industrial and Engineering Chemistry*, Vol. 45, No. 8, Aug. 1953, pp. 1629-1633.
- 7 Longwell, J. P. and Weiss, M. A., "High Temperature Reaction Rates in Hydrocarbon Combustion," *Industrial and Engineering Chemistry*, Vol. 47, No. 8, Aug. 1955, pp. 1634-1643.
- 8 Werle, M. J., "A Critical Review of Analytical Methods for Estimating Control Forces Produced by Secondary Injection: The Two Dimensional Problem," NOLTR-68-5, Jan. 1968, Naval Ordnance Lab., White Oak, Md.
- 9 Shreeve, R. P. and Richmond, J. K., "Design and Operation of the BSRL Pebble Bed Heater—Windtunnel Facility," D1-82-0577, Oct. 1966, Boeing Scientific Research Lab., Seattle, Wash.
- 10 Thayer, W. J., III, "The Two-Dimensional Separated Flow Region Upstream of Inert and Chemically Reactive Transverse Jets," Ph.D. thesis, 1971, Univ. of Washington, Seattle, Wash.; also D1-82-1066, March 1971, Boeing Scientific Research Lab., Seattle, Wash.
- 11 Werle, M. J., Driftmyer, R. T., and Shaffer, D. G., "Two-Dimensional Interaction Experiments—Results of Flowfield and Scale effect Studies," *Proceedings of the 8th Navy Symposium on Aeroballistics*, Naval Ordnance Lab., Vol. 3, 1969, pp. 865-884.
- 12 Thayer, W. J., III, "New Information on the Two-Dimensional Jet Interaction Problem," *AIAA Journal*, Vol. 9, No. 3, March 1971, pp. 539-541.
- 13 Crist, S., Sherman, P. M., and Glass, D. R., "Study of the Highly Underexpanded Sonic Jet," *AIAA Journal*, Vol. 4, No. 1, Jan. 1966, pp. 68-71.
- 14 Spaid, F. W., "A Study of Secondary Injection of Gases into a Supersonic Flow," Ph.D. thesis, June 1964, California Inst. of Technology, Pasadena, Calif.
- 15 Allan, W. L., "An Experimental Investigation of the Aerodynamic Force Characteristics of a Jet Issuing Transverse to a Wedge," F-68-1, JPC-444, NASA CR-96722, Jan. 1968, Purdue Univ., Lafayette, Ind.
- 16 Chapman, D. R., Kuehn, D. M., and Larson, H. K., "Investigation of Separated Flows in Supersonic and Subsonic Streams with Emphasis on the Effect of Transition," TN 3869, 1957, NACA.
- 17 Love, E. S., "Pressure Rise Associated with Shock-Induced Boundary-Layer Separation," TN 3601, 1955, NACA.
- 18 Hahn, J. S., "Experimental Investigation of Turbulent Step-Induced Boundary-Layer Separation at Mach Numbers 2.5, 3, and 4," AEDC-TR-69-1, March 1969, ARO Inc., Arnold Air Force Station, Tenn.